TEMPERATURE-DEPENDENT STRUCTURE AND OPTICAL PROPERTIES OF In$_2$Se$_3$ THIN FILMS

Y. YUAN[a,*], Y. LI[b], Z. WANG[c], H. REN[a], J. LI[b], W. CHEN[a]

[a]Dept. of Electronic Engineering, Center for Intelligent Medical Electronics, Fudan University, 200433, Shanghai,China
[b]Dept. of Optical Science and Engineering, Fudan University, 200433, Shanghai China
[c]Shanghai Institute of Technical Physics of the Chinese Academy of Sciences ,200083, Shanghai China

Chalcogenide-based In$_2$Se$_3$ thin films were deposited by RF magnetron sputtering method at room temperature, and then were annealed at different temperature under nitrogen atmosphere in order to study the effect of annealing temperature on structure and optical. X-ray diffraction analysis show that, the preferred orientation in (110), (006), and (207) plane were observed in XRD result of the film sample annealed at 400℃. The Raman spectrometer result reveals that the main Raman peaks were identified as the γ-phase In$_2$Se$_3$ structure and the peak in the film annealed at 400℃ moves to small direction indicates the inner structure changes occurrence. A Spectroscopic Ellipsometer was employed to measure the optical constants including refractive index and the extinction coefficient of the films. The optical bandgap decreased from 3.41 eV to 2.45 eV with the annealed temperature increasing. The variation is attributed to the Burstein-Moss effect.

1. Introduction

Chalcogenide glass have recently   attracted a lot of attention duo to its unique physical, electrical and optical properties [1-6], Which is including the relatively wide transparency window [7], the photo-induced phenomena [8], the low-energy phonons [9] and the high nonlinear refractive indices [10]. these properties make chalcogenide application in the next generation optoelectronic devices [11-15]. As binary chalcogenide, Indium Selenium as binary chalcogenide is a well-known direct band gap semiconductor [16,17]. which is beneficial for efficient light absorption and detection regarded as a kind of ideal material for radiation detector, switching and photovoltaics [18-22]. Commonly, the thermal treatment influences greatly on the thin films physical properties[23-26]. In addition, the In$_2$Se$_3$ film is a kind of thermal sensitive materials. Therefore, it is necessary to investigate the temperature-dependent physical properties of In$_2$Se$_3$ thin films.

---

[*] Corresponding author: yyf@fudan.edu.cn

In this paper, the In_2Se_3 thin films were deposited by RF magnetron sputtering method at room temperature, and then were annealed at different temperature under nitrogen atmosphere. We discussed the thermal treatment as a tunable tool to affect the properties of In_2Se_3 films and shown the temperature-dependent changes of the structures and optical films.

2. Experimental

The In_2Se_3 thin films were deposited on both fused quartz and Si (100) substrates by the magnetron sputtering method at room temperature. All the substrates were cleaned by using the ultrasonic cleaner under the standard cleaning of process. The In_2Se_3 target purity is about 99.999%. The chamber was evacuated down to approximately 7×10^{-6} mbar. And the working pressure was approximately 2.8×10^{-3} mbar. The sputtering power was controlled at 60 W with RF mode during 30min deposition. The films thickness is about 150 nm. Then, the film samples under the same conditions were annealed under nitrogen atmosphere at 100 ℃, 200 ℃, 300 ℃ and 400 ℃, respectively.

The fabricated In_2Se_3 films were detected by X-ray diffractometer (XRD) (Bruker D8 Advance) with Cu-Kα ($\lambda = 1.54056$ Å) radiation. The diffraction angles were set from 10° to 60° at 0.02° interval each step. The Raman spectra of the films were recorded by Raman micro-spectroscopy (Nanofinder 30). The optical transmission spectra were obtained using a dual light path UV–VIS–NIR (Lambda 1050) spectrophotometer in the wavelength range from 300 nm to 2500 nm. The Spectroscopic Ellipsometer (V-VASE) was employed to obtain the films optical parameters.

3. Results and discussion

The structural features of all the films were analyzed according to the XRD pattern. Fig. 1. shows the XRD patterns of both as-deposited and annealed In_2Se_3 film samples. The absence of structural peaks for as-deposited film confirms the amorphous state of In_2Se_3 as well as the sample at the annealing temperature of 100℃. It indicates different polycrystalline characteristics of remaining samples that the emergence of sharp Bragg diffraction peaks at higher annealing temperature such as 200 ℃, 300 ℃ and 400 ℃. Obviously, the preferential orientation of samples was changed into (102), (110), (006), (202), (116), (207), and (306) peaks at high annealing temperature of 400 ℃ from that of in (006) and (134) peaks at low annealing temperatures including 200 ℃ and 300 ℃. It indicates that the thermal treatment acts as a tunable role affecting two crystalline phases. The observed (006), (207) and (134) peaks were identified as the γ-phase In_2Se_3 structure[27]. All the diffraction peaks correspond well to the hexagonal defect wurtzite structure[28].

As shown in the Fig. 2, the Raman spectra of the films selected can identify that the phase transition of the samples is caused by the annealing effect. The energy range of vibrations extends to 400 cm^{-1} or so and is almost the same for all samples. This indicates the similarity in mass and bond forces among the two elements of In and Se. The main Raman peaks of pure In-Se films are consistent with other works[27]. The peaks at 103 cm^{-1}, 154 cm^{-1} and 307 cm^{-1} are related to the

In-Se phase[29]. The peak in the film annealed at 400 ℃ moves to small direction indicates the inner structure changes occurrence. The strong Raman peak at 154 cm^{-1} is related to the zone center mode of the γ-phase In_2Se_3 crystal. The weaker peak at 248 cm^{-1} is probably attributed to the Se-Se chain. The main Raman peaks were identified as the γ-phase In_2Se_3 structure, which is consistent to the XRD results.
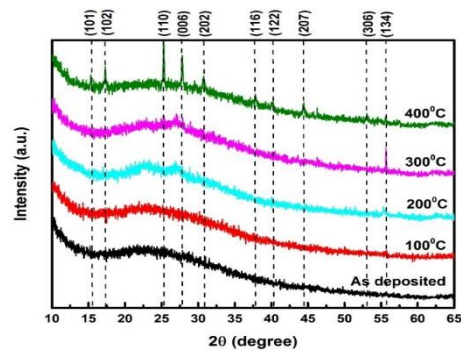

Fig.1. The XRD spectra of the as-deposited and annealed In_2Se_3 films.
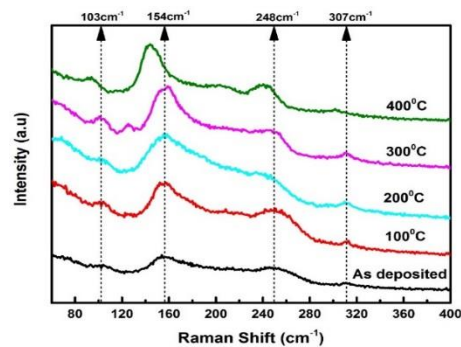

Fig. 2. The Raman spectra for the as-deposited and annealed In_2Se_3 films.

As a function of wavelength, the optical transmission spectra of the as-deposited and annealed In_2Se_3 films is shown in Fig. 3. The spectrum range is from 300 nm to 2500 nm. Obviously, the transmittance spectra of the films varied significantly with the thermal process. It is observed that the transmittance of the films in visible light region is lower than that in the near-infrared light region. The transmission spectrum of the as-deposited film is similar to that of the film sample annealed at 100 ℃. It reflects the absence of phase transition in the annealed sample, which was coincident with the results of Raman and XRD measurements. All of the absorption edges of the films shift toward longer wavelength (red-shift) during the thermal process, which indicates the narrowing of band gap. Moreover, the transmittance is between from 50% to 90% in near-infrared region which allows this chalcogenide glasses to have various applications in infrared fiber optics and other infrared systems [24]. Moreover, it is clearly that thermal treatment can be as an effective mean for tunable of transmittance.
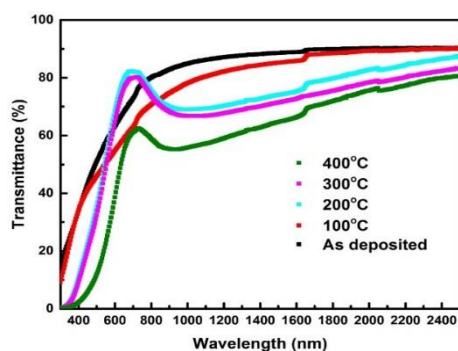
Fig. 3. Transmittance spectra of the as-deposited and annealed In$_2$Se$_3$ films

Both of refractive index (n) and extinction coefficient (k) curves for the as-deposited and annealed In$_2$Se$_3$ films were given in Fig. 4. It is clear that there is an inverse relation between the refractive index (n) and extinction coefficient (k). Moreover, a clear peak in n and k spectra confirms that optical transition energy levels in In$_2$Se$_3$ will appear at around 400 nm. The value of n increases firstly and then decreases in the visible light region. It is increasing in the near in near-infrared region. The value of k decreases firstly and then increases in the visible light region. The n and k in 400 ℃ annealing temperature film are different with other films which is correspond with the different structure. The n has higher values about 3.4-3.8 in the weak absorption region. This may be as a result of the resonance effect between the incident photons and the electron polarization which causes coupling of electrons in the oscillating electromagnetic filed [30]. The high refractive index (n) is good indicators for integrated optics. In near-infrared region, the values of k increases with the wavelength increasing. The study of extinction coefficient (k) is extremely important as the prepared material for application in photo-sensor, photo-electronic, phase transition material, memory devices etc.[31]
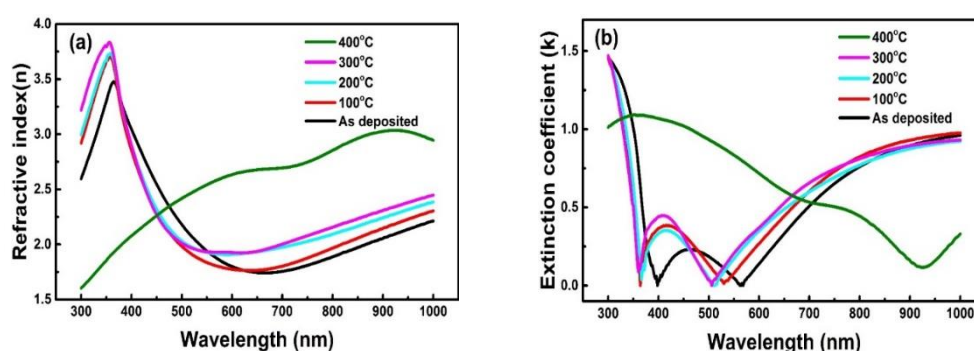

Fig. 4. (a) Refractive index (n) for the films. (b) extinction coefficient (k) for the films.

The absorption coefficient α plays as an important parameter in the constant calculation of semiconductor films. It can be calculated from the extinction coefficient k by the following formula [32]:

$$\alpha = 4\pi k/\lambda \tag{1}$$

As the thickness increase, the energy level seems to be changed which may be due to the incorporation of new energy states or the change of defects. The optical band gap (E_g) of the films can be investigated using Tauc relation [33]:

$$\alpha h\upsilon = A(h\upsilon - E_g)^n \tag{2}$$

where, $h\upsilon$ is the photon energy, A is a constant, n is equal to 1/2 for direct band gap. The optical band gap E_g is obtained by extrapolating the linear portion of the plot to the energy axis. The plot of variation of $(\alpha h\upsilon)^2$ versus $h\upsilon$ is shown in Fig. 5. The obtained values of the optical band gap were listed in Table 1. It is clearly that the decreases from 3.41 eV to 2.45 eV as the annealing temperature increasing. Generally, the dependent of band gap on the thermal process can appear due to a less density of dislocation (structural defects) as the annealing temperature increases [34]. These defects can introduce localized states near the band edges leading to an increase in the band tailing width leading to E_g increases. In other words, the thermal process effect on carrier concentration which is decreases with increasing annealing temperature. The decrease in carrier concentration contributes to the decrease of the optical bandgap which is primarily attributed to the Burstein-Moss effect shift. The Burstein-Moss effect can be written as ΔE_g^{BM} [35]:

$$\Delta E_g^{BM} = \frac{(3\pi^2 n)^{2/3}}{2m_{VC}^*} \tag{3}$$

where n is the carrier concentration and m_{VC}^* is the effective mass. The equation shows that the decrease in carrier concentration and photonic bandgap correlates positively with $n^{2/3}$.

Table 1. The E_g and for the In_2Se_3 films.

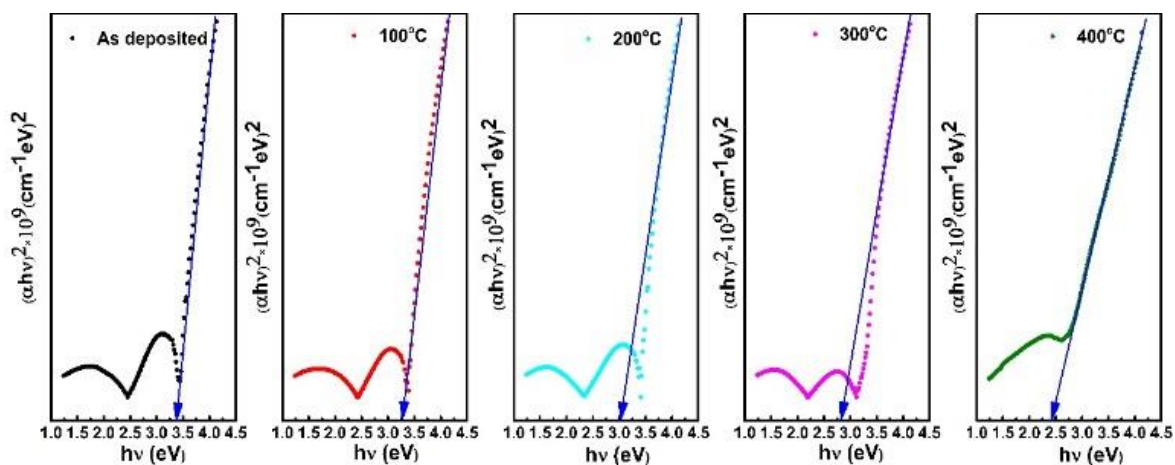| Sample		As deposited	100 ℃	200 ℃	300 ℃	400 ℃
E_g (eV)		3.41	3.25	3.0	2.75	2.45

Fig. 5. The optical band gap of the as-deposited and annealed In_2Se_3 films.

Fig. 6. (a) The real part (ε_r). (b) the imaginary part (ε_i).

For a better understanding the optical properties of the films with different thickness, it is necessary to investigate the dielectric constant. The complex dielectric constant, ε components ($\varepsilon_r = n^2 - k^2$) and ($\varepsilon_i = 2nk$) are related to the optical constants. The real part (ε_r) determines how radiation is refracted while the imaginary part (ε_i) relates to absorption of energy duo to dipole dislocation [36]. Fig. 6 shows the plots of ε_r and ε_i as a function of photon energy. It is obviously that the ε_r have the same behavior as the refractive index (n) due to the lower value of the extinction coefficient compared to the refractive index. The ε_r have similar performance with different annealing temperature, while there was a notable change in ε_i with the increasing of annealing temperature.

4. Conclusions

In this paper, The In2Se3 chalcogenide films were prepared by the magnetron sputtering method and annealed in nitrogen at different temperature. The effect of annealing on the physical properties of the films has been investigated. The XRD analysis shows that the thermal annealing process induces amorphous-crystalline transformation in nature exhibit a hexagonal defect wurtzite crystal structure with preferred orientation in (110), (006) and (207) plane. The Raman results and XRD analysis both confirm the crystalline films as the γ-phase In_2Se_3 structure. The transmittance studies are useful for application in infrared fiber optics and other infrared systems.

The Spectroscopic Ellipsometer analysis reveals that the optical constants can be tunable by the thermal annealing process at different temperatures. The high refractive index (n) is good indicators for integrated optics. The optical band gap decreases from 3.41 eV to 2.45 eV as the increasing annealing temperature. The variation of the optical band gap at different annealing temperature is attributed to the Burstein-Moss effect. Moreover, the In_2Se_3 demonstrates as a promising semiconductor material for photovoltaic application.

Data Availability Statement

The data used to support the findings of this study are available from the corresponding author upon request.

References

[1] M. Buffiere, et al., Energy Technology 7(11), 1900819 (2017).

[2] Y. Yuan et al., The Journal of Physical Chemistry C **122**(11), 6267 (2018).

[3] A. V. Kolobov et al., Nature materials **3**(10), 703 (2004).

[4] M. Grayson et al., Optics express **27**(23), 33606 (2019).

[5] Y. Yuan et al., RSC Advances **7**(73), 46431 (2017).

[6] Y. Yuan et al., Optical Materials Express **7**(11), 4147 (2017).

[7] B. Bureau et al., Journal of Non-Crystalline Solids **345-346**, 276 (2004).

[8] A. Zakery, S. R. Elliott, Journal of Non-Crystalline Solids **330**(1-3), 1 (2003).

[9] Arnaud Zoubir et al., Optics Letters **29**(7), 748 (2004).

[10] H. T. Guo et al., Optics Express **18**(22), 23275 (2010).

[11] Q. Liu, X. Zhao, Journal of Non-Crystalline Solids **356**(44-49), 2375 (2010).

[12] R. Tintu et al., Journal of Applied Physics **108**(7), 073525 (2010).

[13] L. Chen et al., Materials Research Bulletin **70**, 204 (2015).

[14] G. Lenz et al., Optics Letters **25**(4), 254 (2000).

[15] Y. Yuan, J. Li, Electronics Letters **54**(3), 169 (2018).

[16] A. Politano et al., Scientific reports **7**(1), 3445 (2017).

[17] A. A. A. Darwish et al., Applied Surface Science **276**, 210 (2013).

[18] W. Feng et al., Physical chemistry chemical physics : PCCP **17**(5), 3653 (2015).

[19] N. T. Hung et al., Applied Physics Letters **111**(9), 092107 (2017).

[20] H. Ertap et al., Journal of Luminescence **167**, 227 (2015).

[21] B. Tang et al., Nanoscale **11**(27), 12817 (2019).

[22] Han et al., Nanomaterials **9**(9), 1216 (2019).

[23] A. El-Korashy et al., Physica B: Condensed Matter **391**(2), 266 (2007).

[24] H. Nyakotyo et al., Optics & Laser Technology **92**, 182 (2017).

[25] U. Chalapathi et al., Superlattices and Microstructures **103**, 221 (2017).

[26] J. Kaur et al., Phase Transitions **93**(1), 134 (2019).

[27] Y. Yan et al., Materials Letters **109**, 291 (2013).

[28] S. Marsillac et al., Thin Solid Films **288**(1), 14 (1996).

[29] C.-H. Ho et al., Journal of Applied Physics **115**(3), 033501 (2014).

[30] A. S. Hassanien, A. A. Akl, Journal of Alloys and Compounds **648**, 280 (2015).

[31] A. A. Mulama et al., New Journal of Glass and Ceramics **05**(02), 16 (2015).

[32] J. C. Manifacier et al., Journal of Physics E **9**(11), 1002 (1976).

[33] J.Tauc, A.Menth, Journal of Non-Crystalline Solids **8**(10), 569 (1972).

[34] M. I. Abd-Elrahman et al., Materials Science in Semiconductor Processing **18**, 1 (2014).

[35] A. Eshaghi et al., Optik **126**(24), 5610 (2015).

[36] P. Sharma, S. C. Katyal, S. C., Applied Physics B **95**(2), 367 (2009).